Article

Not peer-reviewed version

Programmed Cell Death 1 Ligand 1 Is Essential for Electroacupuncture Mediated Analgesia in the Cerebellum of Fibromyalgia Mice

Hung-Yu Huang , Younbyoung Chae , Ming-Chia Lin , I-Han Hsiao , Hsin-Cheng Hsu , Chien-Yi Ho , Yi-Wen Lin *

Posted Date: 8 January 2026

doi: 10.20944/preprints202601.0557.v1

Keywords: fibromyalgia; electroacupuncture; PD-L1; TRPV1; neutralization; cerebellum

Article

Programmed Cell Death 1 Ligand 1 Is Essential for Electroacupuncture Mediated Analgesia in the Cerebellum of Fibromyalgia Mice

Hung-Yu Huang [1,2], Younbyoung Chae [3], Ming-Chia Lin [4], I-Han Hsiao [5,6], Hsin-Cheng Hsu [7], Chien-Yi Ho [8,9,10,11] and Yi-Wen Lin [1,12,*]

[1] Graduate Institute of Acupuncture Science, College of Chinese Medicine, China Medical University, Taichung 404328, Taiwan
[2] Department of Neurology, China Medical University Hospital, Taichung 404327, Taiwan
[3] Acupuncture and Meridian Science Research Center, Kyung Hee University, Seoul 02453, Republic of Korea
[4] Department of Nuclear Medicine, E-DA Hospital, I-Shou University, Kaohsiung 82445, Taiwan
[5] School of Medicine, College of Medicine, China Medical University, Taichung 404328, Taiwan
[6] Department of Neurosurgery, China Medical University Hospital, Taichung 404327, Taiwan
[7] Department of Traditional Chinese Medicine, China Medical University Hsinchu Hospital, Hsinchu 302233, Taiwan
[8] Department of Biomedical Imaging and Radiological Science, China Medical University, Taichung 404328, Taiwan
[9] Division of Family Medicine, China Medical University Hsinchu Hospital, Hsinchu 302233, Taiwan
[10] Physical Examination Center, China Medical University Hsinchu Hospital, Hsinchu 302233, Taiwan
[11] Department of Medical Research, China Medical University Hsinchu Hospital, Hsinchu 302233, Taiwan
[12] Chinese Medicine Research Center, China Medical University, Taichung 404328, Taiwan
* Correspondence: yiwenlin@mail.cmu.edu.tw

Abstract

Background: Fibromyalgia is a chronic disease that predominantly affects women and lasts over several months, causing problems both to individuals and society. While several studies have demonstrated the potential of electroacupuncture (EA) to alleviate fibromyalgia pain in mice, further research is needed to investigate its underlying mechanisms. Programmed cell death ligand-1 (PD-L1)/PD-1 was first identified to be involved in cancer immunotherapy, but its application to pain management has not been yet investigated. **Methods:** This study aimed to explore the mechanism underlying action of PD-L1 on PD-1 pathway in a mouse model of fibromyalgia. **Results:** We established such a mouse model using intermittent cold stress (ICS) and confirmed mechanical (D4: 2.02 ± 0.13 g, $n = 9$) and thermal (D4: 4.28 ± 0.21 s, $n = 9$) hyperalgesia. We found that EA, intracerebral ventricle (ICV) PD-L1 injection, or *transient receptor potential vanilloid 1* (*Trpv1)* knockout effectively counteracted hyperalgesia. We observed low PD-1 expression in the cerebellum of fibromyalgia mice but increased expression of TRPV1 and pain-related kinases. These phenomena could be further reversed by EA, ICV PD-L1 injection, and *Trpv1* knockout. To confirm that these effects were caused by PD-L1 release, we added PD-L1 neutralizing antibodies to the EA and PD-L1 treatment. The analgesic effects and EA and PD-L1 mechanisms were inhibited. **Conclusions:** Our results elucidate the role of the PD-L1/PD-1 pathway in EA treatment of fibromyalgia and reveal its potential value for fibromyalgia.

Keywords: fibromyalgia; electroacupuncture; PD-L1; TRPV1; neutralization; cerebellum

 doi:10.20944/preprints202601.0557.v1

1. Introduction

Programmed cell death protein 1 (PD-1), first discovered in 1992, is a membrane protein expressed on T cells and primarily involved in apoptosis. Its structure is mainly composed of 288 amino acids, including an N-terminal domain. PD-1 is also present on the cell membranes of T lymphocytes, B lymphocytes, and natural killer cells [1]. Recent reports indicate that the main function of PD-1 is regulating T cell activity in tissues to control cancer cells. Cancer cells can suppress the immune system, making T cells unable to kill them. This process is mediated by PD-1. When PD-1 is expressed on the surface of T cells, the PD-L1 expressed on the surface of cancer cells binds to PD-1, inhibiting it [2]. However, in acute and chronic pain models, PD-L1 and PD-1 binding is involved in pain relief [3]. Therefore, studying the PD-L1/PD-1 pathway and its related pathways is even more important in fibromyalgia (FM) models.

Clinical diagnosis of FM currently lacks standardization, relying primarily on physician subjective judgment. While numerous questionnaires can help assess the symptoms and severity of FM, scientifically validated data are still lacking. FM is a chronic pain disorder affecting numerous social aspects, including personal, healthcare, and economic. FM is more common in women and frequently accompanied by tension headaches, irritable bowel syndrome, anxiety, and depression. Women generally have a significantly lower pain threshold than men and experience more severe symptoms [4]. Currently, there is no effective cure for FM; medications can only relieve symptoms. Novel therapeutic strategies for FM involve use of specific circulating microRNAs [5]. Nonpharmacological options, such as noninvasive brain stimulation, exercise, yoga, acupuncture, and nutritional therapy, are being explored to alleviate symptoms and improve quality of life [6]. FM is caused by repeated central nervous system activation, in what is known as central sensitization. The incidence of FM is about 2–8%, and its etiology and pathogenesis are not fully understood. Recent studies have indicated that inflammatory cytokines may damage neural circuits, leading to central sensitization and neuroinflammation [7].

Acupuncture has been used in Asia for over 3000 years. In recent years, acupuncture has been optimized to treat many diseases. The WHO recognizes acupuncture as applicable to over 100 diseases, particularly for pain management. Acupuncture is a method for balancing the flow of Qi and blood and promoting health of the body's meridians. Western medicine has accepted that acupuncture can relieve symptoms by stimulating peripheral nerves, connective tissues, and muscles [8]. Particularly, electroacupuncture (EA) could enhance anti-inflammatory effects and effectively control inflammation in a mouse sepsis model [9]. Recent studies reported that EA can effectively stimulate the vagal-adrenal axis in mice by stimulating the ST36 acupoint [10]. Similarly, our previous research showed that EA can release adenosine triphosphate, interleukin 1β (IL-1β), and IL-6 at local acupoints [11]. Further evidence show that EA can treat inflammatory pain [12,13], neuropathic pain [14], and FM pain [15–17]. Neuroinflammation plays an increasingly important role in the brain and is associated with many diseases [18]. In addition, EA can treat pain and depression comorbidities by reducing inflammatory factors in the plasma such as ILs, tumor necrosis factor-alpha (TNF-α) and interferon gamma (IFN-γ) [19].

Based on the above, we next wanted to investigate whether EA could treat the mechanical and thermal hyperalgesia caused by intermittent cold stress (ICS)-induced FM pain, whether EA analgesia was related to PD-L1/PD-1, and the effect of PD-L1/PD-1 on the TRPV1 signaling pathway. First, we established a mouse FM model using ICS, which successfully induced mechanical and thermal hyperalgesia in mice and EA could alleviate. EA could reverse the significant changes observed in the expression levels of PD-L1/PD1 and related molecules in the mouse cerebellum. Similar results were found in mice receiving PD-L1 injection or with *Trpv1* deletion. To confirm that EA can relieve pain by increasing PD-L1, we administered PD-L1 neutralizing antibodies during EA or ICV PD-L1 injection; both the analgesic effect and the involved molecular mechanisms were attenuated. Therefore, our findings suggest that the analgesic effect of EA may be related to TRPV1 signaling regulation by PD-L1/PD1 in the mouse cerebellum. Accordingly, we propose that EA can modulate PD-L1/PD1 signaling, being useful for treating FM.

 doi:10.20944/preprints202601.0557.v1

2. Results

2.1. Intermittent Cold Stress Successfully Induced Mechanical and Thermal Hyperalgesia Alleviated by EA, ICV PD-L1, or Trpv1 Deletion

To assess the functional mechanisms underlying FM, we first established a mouse model of FM using ICS. In wild-type mice, the von Frey test showed normal mechanical pain thresholds at baseline (Figure 1A, black column, day 0: 4.13 ± 0.16 g, n = 9). On Days 3 (Figure 1A, red column, day 3: 1.93 ± 0.12 g, n = 9) and 4 (Figure 1A, red column, day 4: 2.02 ± 0.13 g, n = 9) in FM mice, we observed significant mechanical hypersensitivity. Administering EA (Figure 1A, blue column, day 4: 3.83 ± 0.11 g, n = 9) or ICV PD-L1 injection (Figure 1A, green column, day 4: 3.72 ± 0.19 g, n = 9) to FM mice resulted in strong analgesic effects. Similar results were observed in *Trpv1*$^{-/-}$ mice (Figure 1A, gray column, day 4: 3.69 ± 0.21 g, n = 9). We further used the Hargreaves' test to examine thermal hypersensitivity. All groups had normal thermal pain thresholds. On Days 3 (Figure 1B, red column, day 3: 4.04 ± 0.32 s, n = 9) and 4 (Figure 1B, red column, day 4: 4.28 ± 0.21 s, n = 9), FM mice exhibited thermal hyperalgesia, which persisted for two days. Notably, EA (Figure 1B, blue column, day 4: 7.86 ± 0.20 s, n = 9) or ICV PD-L1 injection (Figure 1B, green column, day 4: 7.19 ± 0.26 s, n = 9) significantly reduced pain hypersensitivity. To explore the relationship between PD-L1 and TRPV1 in FM, we also induced ICS in *Trpv1*$^{-/-}$ mice. However, thermal hypersensitivity was not induced in *Trpv1*$^{-/-}$ mice on days 4 (Figure 1B, gray column, day 4: 7.48 ± 0.29 s, n = 9).

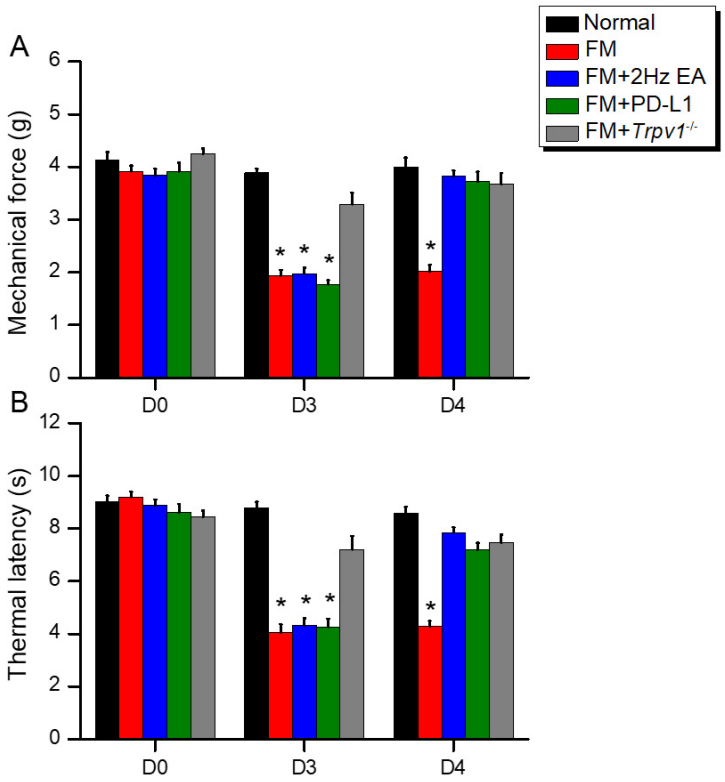

Figure 1. Diagram characterizing mechanical and thermal hyperalgesia in mice. (A) von Frey filament test indicating the mechanical threshold and (B) Hargreaves' test for thermal latency. * significant difference compared to the normal group in the same day. n = 9 per group.

2.2. PD-1 Was Attenuated and Nociceptive TRPV1 Signaling Increased in the CB5 Region of FM Mice: These Phenomena Were Reversed by EA, ICV PD-L1 Injection, or Trpv1 Deletion

We first investigated PD-1 expression in the CB5 region of mice after ICS-induced FM. Western blot results showed that wild-type mice had normal PD-1 protein levels in the CB5 region (Figure 2A,

 doi:10.20944/preprints202601.0557.v1

black column, day 4: 100.00 ± 1.2%, n = 6), while ICS-induced FM mice showed a significant reduction in expression (Figure 2A, red column, day 4: 66.25 ± 3.53%, n = 6). EA (Figure 2A, blue column, day 4: 99.59 ± 2.59%, n = 6) or ICV PD-L1 (Figure 2A, green column, day 4: 99.89 ± 2.81%, n = 6) injection significantly increased PD-1 protein levels in the CB5 region of mice, as observed in *Trpv1*$^{-/-}$ mice (Figure 2A, gray column, day 4: 93.62 ± 2.26%, n = 6. Furthermore, on Day 4 after ICS-induced FM pain, TRPV1 concentration in the CB5 region of FM mice was significantly increased (Figure 2A, black column, day 4: 140.99 ± 9.20%, n = 6). EA (Figure 2A, blue column, day 4: 97.90 ± 4.29%, n = 6) or ICV PD-1 injection (Figure 2A, green column, day 4: 98.81 ± 3.77%, n = 6) inhibited TRPV1 overexpression in the CB5 region; in mice with *Trpv1* deletion, TRPV1 protein almost disappeared. Next, we observed a significant increase in the levels of proteins involved in downstream pPI3K/pAkt/pmTOR pathways (Figure 2A, black columns, n = 6). Similarly, EA (Figure 2A, blue columns, n = 6), ICV PD-1 injection (Figure 2A, green columns, n = 6) and *Trpv1* deletion (Figure 2A, gray columns, n = 6) effectively inhibited overexpression of pPI3K/pAkt/pmTOR signaling mediators. Compared with normal mice, FM mice showed a relative increase in functional phosphorylation of pERK, pp38, and pJNK (Figure 2A, red columns, n = 6). In ICS-induced EA (Figure 2A, blue columns, n = 6) or ICV-injected PD-L1 mice (Figure 2A, green columns, n = 6), phosphorylation was reduced, while *Trpv1*$^{-/-}$ mice showed normal pERK, pp38, and pJNK levels after ICS induction (Figure 2A, gray columns, n = 6).

Next, we moved to transcription factors; Western blot results showed normal pNFκB and pCREB expression in the CB5 region of wild-type mice, and significantly increased expression in FM mice (Figure 2A, red columns, n = 6). In the EA (Figure 2A, blue columns, n = 6) or PD-L1 groups (Figure 2A, green columns, n = 6), pNFκB and pCREB expression was significantly reduced, similarly to what was observed in *Trpv1*$^{-/-}$ mice (Figure 2A, gray columns, n = 6). We further investigated a possible role for the Nav1.7 or Nav1.8 nociceptive channels. Our data indicated higher activity of both these ion channels after induction (Figure 2A, red columns, n = 6). In EA (Figure 2A, blue columns, n = 6), PD-L1 (Figure 2A, green columns, n = 6), or *Trpv1*$^{-/-}$ groups, the overexpression was reduced. Immunofluorescence staining showed normal PD-1 expression in the CB5 region, which decreased after FM induction (Figure 2B, n = 3). In EA, PD-L1, and *Trpv1*$^{-/-}$ groups (Figure 2B, n = 3), the number of PD-1 immune granules in the CB5 cell layer increased. Conversely, the quantity of pERK was normal, but enhanced in FM mice. pERK overexpression was attenuated in mice stimulated with EA, PD-L1, as well as in *Trpv1*$^{-/-}$ mice (Figure 2B, n = 3).

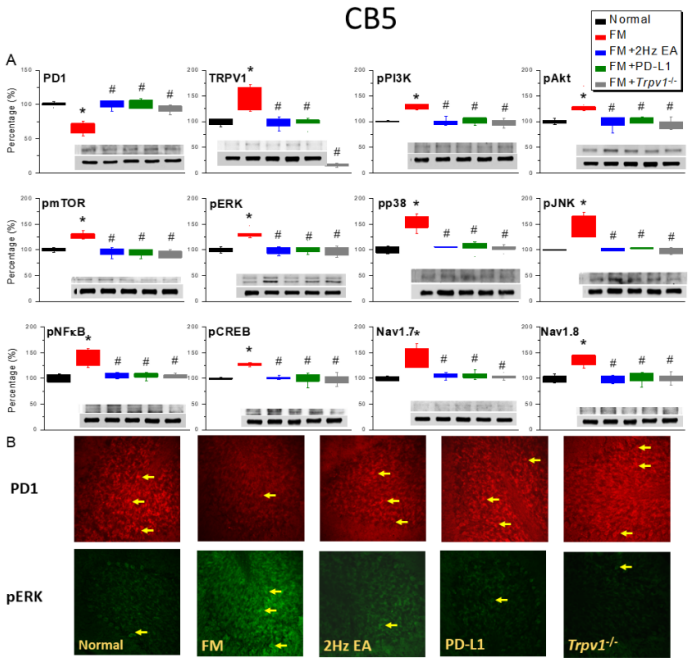

 doi:10.20944/preprints202601.0557.v1

Figure 2. EA, ICV PD-L1 injection, and *Trpv1*$^{-/-}$ increase PD-1 and decrease TRPV1 pathway in the CB5 of FM mice (A) Western blot indicates that EA, PD-L1, *Trpv1*$^{-/-}$ noticeably increases PD-1 and decreases TRPV1 pathway. (B) Immunofluorescence staining for PD-1 (red) and pERK (green) in fibromyalgia mice. $^{*}p < 0.05$ vs. normal group. $^{\#}p < 0.05$ vs. FM group. FM = fibromyalgia (per group, n = 6 in Western blot, n = 3 in immunofluorescence staining).

2.3. Effects of EA, ICV PD-L1 Injection, and Trpv1 Deletion on Cold Stress-Induced Fibromyalgia Pain in the CB6 and CB7

Next, we evaluated PD-1 expression in the CB6 and CB7 region after inducing FM. In a Western blot, PD-1 content in both regions of FM mice relatively decreased compared to normal (CB6: Figure 3A, red column, day 4, 75.49 ± 2.35 %, $n = 6$; CB7: Figure 4A, red column, day 4, 82.76 ± 3.56 %, $n = 6$), increasing by EA (CB6: Figure 3A, blue column, day 4, 98.18 ± 4.19 %, $n = 6$; CB7: Figure 4A, blue column, day 4, 101.11 ± 2.61 %, $n = 6$) or ICV PD-1 injection (CB6: Figure 3A, green column, day 4, 98.45 ± 2.77 %, $n = 6$; CB7: Figure 4A, green column, day 4, 99.77 ± 2.12 %, $n = 6$) in the CB6 and CB7 region. Compared with the FM group, the PD-1 receptors in *Trpv1*$^{-/-}$ mice reached similar levels to the normal group on Day 4 after FM (CB6: Figure 3A, gray column, day 4, 100.23 ± 3.82 %, $n = 6$; CB7: Figure 4A, gray column, day 4, 102.73 ± 2.43 %, $n = 6$). We then investigated the effect of PD-1 on TRPV1. Compared with normal mice, TRPV1 expression in the CB6 and CB7 region of FM mice significantly increased (CB6: Figure 3A, red column, day 4, 138.17 ± 4.57 %, $n = 6$; CB7: Figure 4A, red column, day 4, 139.76 ± 4.85 %, $n = 6$), an effect attenuated by EA (CB6: Figure 3A, blue column, day 4, 99.25 ± 2.80 %, $n = 6$; CB7: Figure 4A, blue column, day 4, 96.18 ± 3.28 %, $n = 6$) or ICV PD-L1 injection (CB6: Figure 3A, green column, day 4, 97.65 ± 2.27 %, $n = 6$; CB7: Figure 4A, red column, day 4, 97.73 ± 2.04 %, $n = 6$). As expected, almost no TRPV1 protein expression was observed in *Trpv1*$^{-/-}$ mice. Another Western blot showed significant overexpression of downstream TRPV1 molecules (such as pPI3K/pAkt/pmTOR) in the CB6 (Figure 3A, red column, $n = 6$) and CB7 (Figure 4A, red column, $n = 6$) region of FM mice. Conversely, significant pPI3K/pAkt/pmTOR inhibition was observed in the EA or PD-L1 treatment groups (Figure 3 & 4A, blue and green columns, $n = 6$). Compared with FM mice, the pPI3K/pAkt/pmTOR signaling was not enhanced in CB6 & 7 *Trpv1*$^{-/-}$ mice (Figure 3&4A, gray columns, $n = 6$).

We then explored the involvement of pERK, pp38, and pJNK in the CB6 and CB7 region of FM mice. Their expression was significantly increased in FM mice (Figures 3 and 4A, red columns, $n = 6$) and attenuated in mice treated with EA (Figures 3 and 4A, blue columns, $n = 6$), ICV PD-L1 injection (Figures 3 and 4A, green columns, $n = 6$), as well as in *Trpv1*$^{-/-}$ mice (Figures 3 and 4A, gray columns, $n = 6$). Similarly, pNFκB and pCREB expression significantly increased in the CB6 and CB7 region of FM mice (Figures 3 and 4A, red columns, $n = 6$). An effect mitigated in in mice treated with EA, ICV PD-L1 injection, as well as in *Trpv1*$^{-/-}$ mice (Figures 3 and 4A, blue, green, and gray columns, $n = 6$). Similar results were obtained for Nav1.7 and Nav1.8 pain receptor channels. Immunofluorescence staining showed PD-1 positive cells in the CB6 and CB7 region of normal mice, but the number of PD-1 positive cells was significantly reduced in FM mice. EA, ICV PD-L1 injection, and *Trpv1* deletion restored the number of PD-1 positive cells (Figures 3 and 4B, $n = 3$). Further, qualitative analysis showed a significant increase in the number of pERK positive cells in the CB6 and CB7 region of FM mice, similar to the trend observed in Western blot. In contrast, the number of pERK positive cells decreased in mice treated with EA, ICV PD-L1 injection, and *Trpv1* deletion (Figures 3 and 4B, $n = 3$).

2.4. ICV PD-L1 Neutralizing Antibodies Reversed the Analgesic Effects of EA or PD-L1 in Fibromyalgia Mice

In normal mice, regular mechanical and thermal pain thresholds were observed on Days 0 and 4 (Figure 5A, black column, day 0: 3.98 ± 0.17 g, day 4: 4.19 ± 0.33 g, $n = 9$). Further results showed that mice receiving the ICS model exhibited significant mechanical (Figure 5A, red column, day 4: 2.10 ± 0.16 g, $n = 9$) and thermal hyperalgesia (Figure 5B, red column, day 4: 4.13 ± 0.46 s, $n = 9$). After ICV injection of PD-1 neutralizing antibodies, the analgesic effect of EA on both mechanical or

 doi:10.20944/preprints202601.0557.v1

thermal hyperalgesia significantly decreased indicating that PD-L1 plays a crucial role in EA analgesia (Figure 5A, blue column, day 0: 3.98 ± 0.17 s, day 4: 4.19 ± 0.33 g, n = 9; Figure 5B, blue column, day 4: 5.23 ± 0.32 s, n = 9). Similarly, on Day 4 after ICS induction, the analgesic effect of ICV PD-1 injection in mechanical and thermal pain diminished due to the PD-L1 neutralizing antibodies (Figure 5A, green column, day 4: 2.43 ± 0.14 g, n = 9; Figure 5B, green column, day 4: 5.95 ± 0.37 s, n = 9).

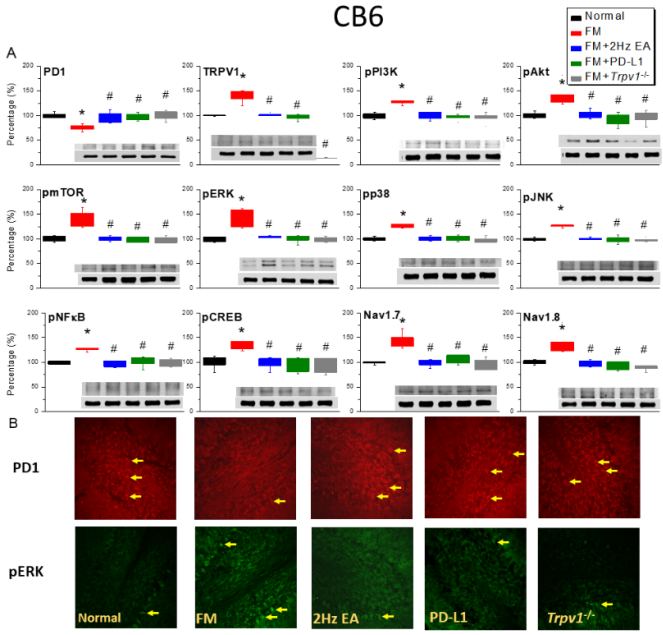

Figure 3. Low PD-1 expression in the CB6 of ICS-induced FM mice. (A) Relative PD-1 and TRPV1 pathway with protein expression in all groups, as indicated by Western blot analysis. (b) Immunofluorescence for PD-1 (red) and pERK (green) expression in five experimental groups. *significant difference between normal and others. #considerable difference between FM and other groups. All results are representative of ≥6 independent experiments for Western blot and three for immunofluorescence staining.

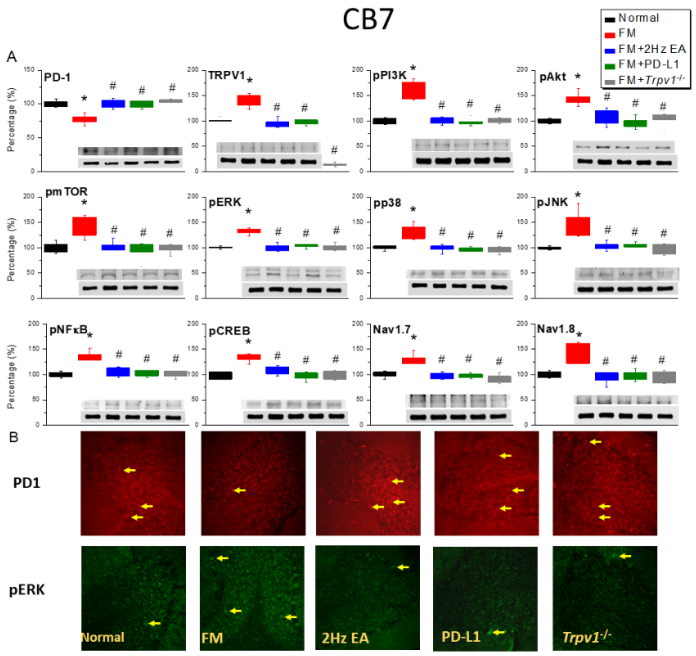

 doi:10.20944/preprints202601.0557.v1

Figure 4. PD-1/TRPV1 interaction is responsible for nociception of ICS-induced FM pain. Protein concentration of PD-1 and TRPV1 related molecules in the CB7 area of mice. Western blotting contained five lanes: Normal, FM, FM + EA, FM + PD-L1, and FM + *Trpv1*$^{-/-}$. (A) PD-1 and TRPV1 associated protein expression (B) Immunofluorescence for PD-1 (red) and pERK (green) expression in all groups. * important variance between normal and others. # extensive modification between FM and other groups. n = 6 independent experiments for Western blot and n = 3 for immunofluorescence staining.

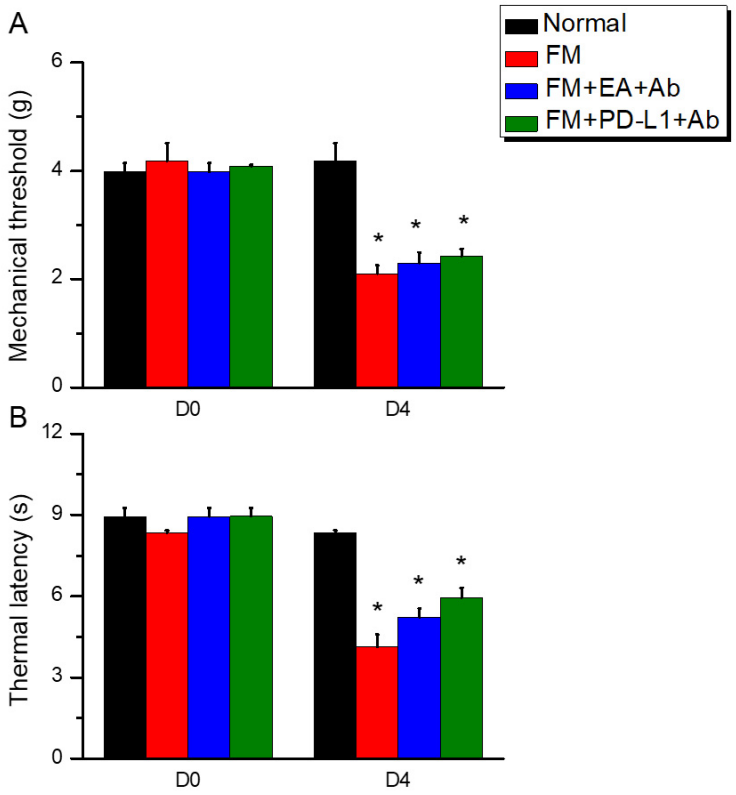

Figure 5. Administration of a PD-L1 neutralizing antibody attenuated 2Hz EA, PD-L1, or *Trpv1*$^{-/-}$ analgesia. (A) von Frey filament test indicating the mechanical threshold (B) Hargreaves' test for the thermal latency. *significant difference in comparison to the normal group. n = 9 per group.

2.5. The Analgesic Effect of EA or PD-L1 Injection Was Reversed by PD-L1 Neutralizing Antibody Injection

To further confirm the analgesic mechanism of EA or PD-L1 on nociceptive transduction in FM mice, we detected the protein expression levels of the aforementioned molecules in CB5–7 regions. PD-1 levels in the CB5–7 regions significantly decreased in mice with ICS-induced FM (Figures 6–8A, red columns, n = 6). In mice administered with EA and concurrent ICV injection of a PD-L1 neutralizing antibody, we observed a decrease in PD-1 concentration, indicating that PD-L1/PD-1 is the mediator of EA analgesia (Figures 6–8, blue columns, n = 6). Similar results were observed in mice simultaneously injected with PD-L1 and PD-L1 antibodies (Figures 6–8, green columns, n = 6). Furthermore, ICS enhanced TRPV1 and pPI3K/pAkt/pmTOR signaling, as indicated by the elevated levels of mediators in the CB5–7 regions (Figures 6–8B–E, red columns, n = 6). Similar increases were observed in mice simultaneously receiving EA (Figures 6–8B–E, blue columns, n = 6) or PD-L1 injection and PD-L1 antibody injection (Figures 6–8B–E, green columns, n = 6). Following ICS induction, pERK/pp38/pJNK levels significantly increased in these regions (Figures 6–8F–H, red columns, n = 6). Similar results were observed in mice receiving EA (Figures 6–8F–H, blue columns, n = 6) or PD-L1 treatment (Figures 6–8F–H, green columns, n = 6) concurrently with PD-L1 antibody

 doi:10.20944/preprints202601.0557.v1

injection. The expression of pNFκB and pCREB proteins significantly increased in both mice receiving ICS, EA and PD-L1 injection (Figures 6–8I,J, $n = 6$) concurrently with PD-L1 antibody injection. Similar increases in expression were observed in Nav1.7 and Nav1.8 (Figures 6–8I,J, $n = 6$).

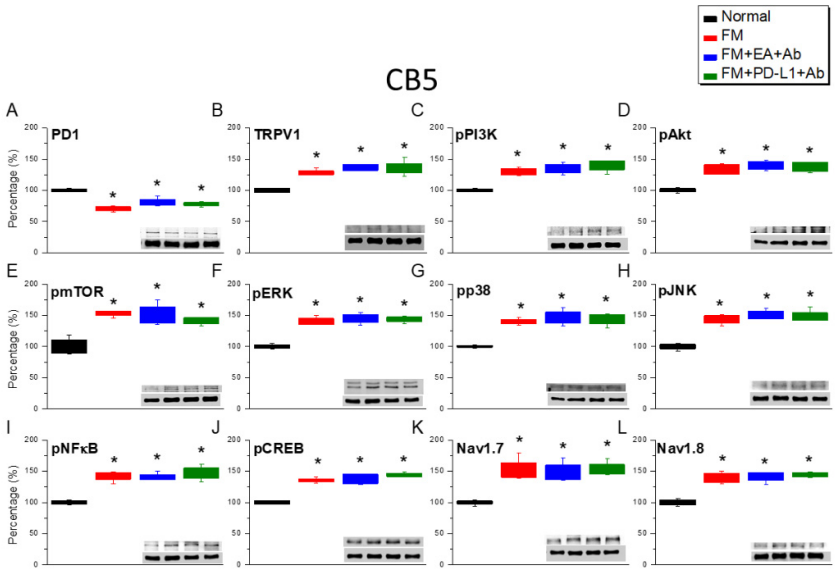

Figure 6. Protein levels of PD-1 and TRPV1 associated molecules in the CB5 of mice. Western blotting contained four lanes: Normal, FM, FM + EA +Ab, FM + PD-L1 + Ab groups. (A) PD-1, (B) TRPV1, (C) pPI3K, (D) pAkt, (E) pmTOR, (F) pERK, (G) pp38, (H) pJNK, (I) pNFκB, (J) pCREB, (K) $Na_v1.7$, and (L) $Na_v1.8$. *significant difference between normal and others. n = 6.

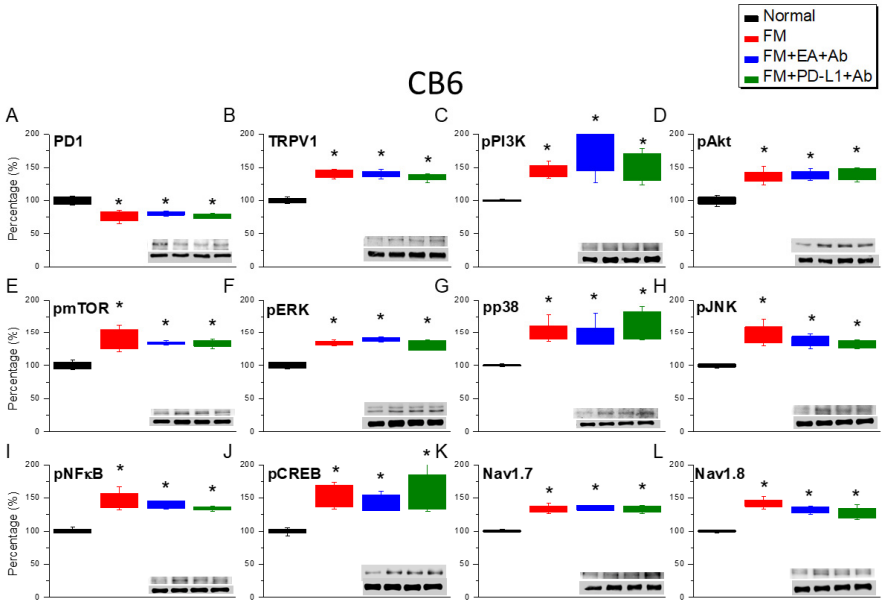

 doi:10.20944/preprints202601.0557.v1

Figure 7. Protein levels of PD-1 and TRPV1 associated molecules in the CB6 of mice. Western blotting contained four lanes: Normal, FM, FM + EA +Ab, FM + PD-L1 + Ab groups. (A) PD-1, (B) TRPV1, (C) pPI3K, (D) pAkt, (E) pmTOR, (F) pERK, (G) pp38, (H) pJNK, (I) pNFκB, (J) pCREB, (K) $Na_v1.7$, and (L) $Na_v1.8$. *significant difference between normal and others. n = 6.

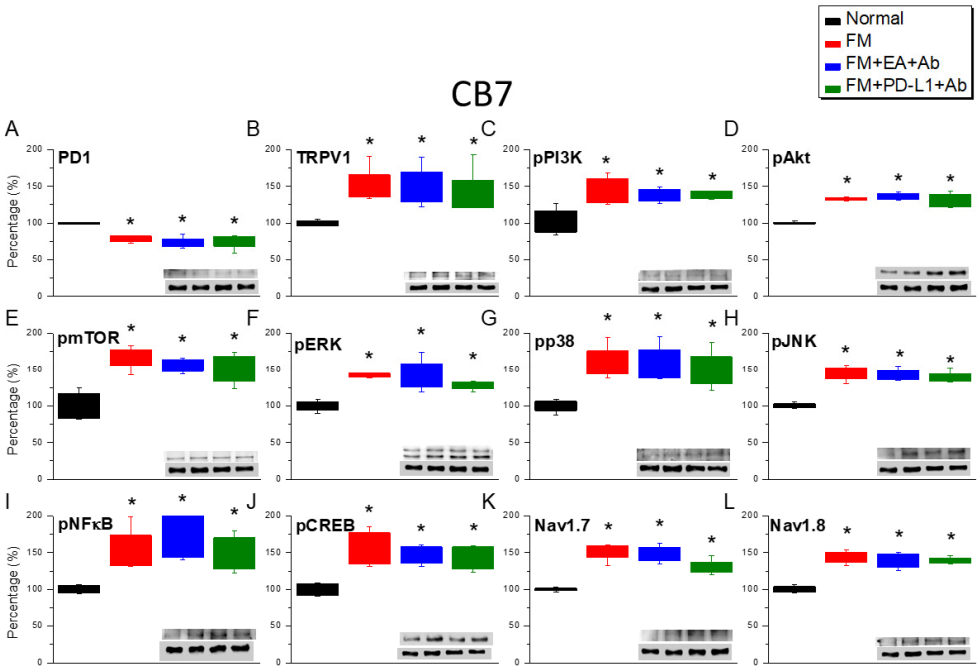

Figure 8. Protein expression of PD-1 and TRPV1 associated molecules in the CB7 of mice. Western blotting contained four lanes: Normal, FM, FM + EA + Ab, FM + PD-L1 + Ab groups. (A) PD-1, (B) TRPV1, (C) pPI3K, (D) pAkt, (E) pmTOR, (F) pERK, (G) pp38, (H) pJNK, (I) pNFκB, (J) pCREB, (K) $Na_v1.7$, and (L) $Na_v1.8$. *significant difference between normal and others. n = 6.

3. Discussion

The present study is the first to offer evidence that the modulatory effect of EA analgesia is mediated by PD-1 signaling in the cerebellum of FM mice. Our results identified a decrease in PD-1 receptor expression in the cerebellum after ICS-induced FM and simultaneous increase in nociceptive TRPV1 signaling. In contrast, EA, PD-L1 injection, and *Trpv1* deletion exert an antinociceptive effect which increased PD-1 expression in the cerebellum. Our data indicate FM pain suppression is mediated b diminished TRPV1 signaling. In fact, the analgesic effect of EA and PD-L1 were abrogated by PD-L1 neutralizing antibody injection.

Recent work indicated that dysfunctional pain regulation is a trademark of FM and indicated that exercise is a proper therapeutic remedy. They performed a 15-week mediation of strengthening exercises and suggested that FM patients had a decline of pain sensation, FM severity and depression. A subgroup receiving functional magnetic resonance imaging in the course of counting thumbnail pressure pain stimulations. Their results showed a noteworthy therapeutic effect of exercise within the left dorsolateral prefrontal cortex and caudate. They also indicated an increased neuronal connection from caudate to cerebellum in the FM patients [20]. Kim et al. showed increased connections within the cerebellum of FM patients as well as more extensive connections in the frontal lobe than the normal group. In FM patients, they also found, via spectral partitioning, a lower

 doi:10.20944/preprints202601.0557.v1

connection to medial prefrontal and its gray matter volume was related to the severity of depression [21]. Mosch et al. indicated, by using voxel-based morphometry (VBM) and diffusion-tensor imaging, revealed decreased gray matter (GM) sizes in parahippocampal gyrus, dorsal anterior cingulate cortex (dACC), putamen, and left dorsolateral prefrontal cortex (DLPFC) in FM patients. In dissimilarity, significant augmented GM volume was detected in cerebellum and thalamus [22].

Recent article, by using VBM analysis, revealed that the GM volume of the cerebellum was considerably enlarged in FM patients compared with normal patients. The altered resting-state functional connectivity was abnormal in cortico–striato–thalamo–cortical circuit in FM patients. The lower function designating irregular reward, mood, decision, and motivation. The amplified GM volume in the cerebellum specified the contribution of cerebellum in the irregular pain sensation in FM patients [23]. A recent paper reported that FM pain was accompanied by increased inflammatory mediators and toll-like receptor 4 (TLR4) signaling pathway in the mouse hypothalamus, periaqueductal gray, and cerebellum. Expression of TLR4 and downstream molecules including MyD88, TRAF6, pERK, pp38, and pJNK was increased in FM mice. An effect inhibited by 2 Hz EA treatment. The additional consequences indicated that activation of TLR4 by lipopolysaccharide considerably convinced FM pain and then reversed by a TLR4 antagonist. This information evidences EA analgesia via TLR4 pathway [24].

PD-L1/PD-1 is a newly developed immunotherapy that can be used for many types of cancer, but there is a lack of evidence for its use in the treatment of pain. PD-1 receptors were generally expressed in the brain neurons; it is unmet to develop PD-1 especially in analgesic peptides that had shown noteworthy beneficial effect with lower adverse properties. Recently, increased PD-L1 to activate PD-1 were reported to moderates neuronal excitability and delivered antinociceptive effects indicating its promising goal for pain relief [25–27]. It is worth noting that Zhao et al. has developed a new small molecule, peptide H-20 that can activate PD-1 to achieve analgesic effects. Their in vitro results revealed that H-20 can bind to PD-1 with μM affinity to activate Src homology 2 domain–containing tyrosine phosphatase 1 (SHP-1) phosphorylation that attenuated painful signals in the mice dorsal root ganglion (DRG). Pretreatment mice with H-20 successfully mitigated pain in normal mice. Intrathecal injection of H-20 showed significant anti-nociception in formalin, acetic acid, and CFA-initiated inflammatory pain models [28]. An excellent recent literature review pointed out that PD-L1/PD-1 route in DRG, sciatic nerve, and spinal cord delivered a chief role in several pain models. Exogenous PD-L1 activation actually attenuated pain symptoms in bone cancer pain mice. They also suggest that PD-L1 significantly increased the infiltration of macrophages into damaged nerve for pain relief. Augmentation of PD-L1/PD-1 in trigeminal ganglia neurons inhibits migraine pain [29].

4. Materials and Methods

4.1. Animals and Fibromyalgia Pain Induction

Mouse experiments were approved by the Institute of Animal Care and Use Committee of China Medical University (Permit no. CMUIACUC-2024-076), Taiwan, following the Guide for the use of Laboratory Animals (National Academy Press). We selected 8–12-week-old female C57B/L6 wild-type mice, purchased from BioLasc Taiwan Ltd. (Yilan, Taiwan), weighing approximately 18–22 g. Animals were directly transported and housed in a specific pathogen free environment; all mice had healthy coats and no wounds. Upon arrival, mice were immediately placed in an environment under a 12-h light/dark cycle (6:00 AM to 6:00 PM), at a room temperature of 25ºC and a humidity of ~60%. To estimate the sample size requirements, we used G*Power 3.1.9.7 program so that each group contained nine mice to achieve a significance level of α = 0.05 and a statistical power of 80%. Mice were randomly assigned to five groups: a normal group (Normal); a cold stress-induced FM group (FM); FM mice treated with 2 Hz EA (FM + 2 Hz EA); FM mice treated with intraventricular PD-L1 injection (FM + PD-L1); and *Trpv1*$^{-/-}$ mice with FM induction (FM + *Trpv1*$^{-/-}$). To initiate FM pain, mice were placed in a 4ºC environment, while the normal group was maintained at a constant temperature of 25ºC. At 10 a.m. the following day, these FM mice were moved back to 25º for 30 min, before

 doi:10.20944/preprints202601.0557.v1

transfer back to 4ºC for 30 min. This process was continued for 6 h until 4 p.m., before they were repositioned again overnight from 4 p.m. over the first three days.

4.2. Electroacupuncture

For EA, mice were anesthetized with 5% isoflurane for induction and 1% isoflurane for maintenance. Two 1-inch stainless steel needles 32G, Yu Kuang Chem. Ind. Corp., Taiwan) were inserted perpendicularly to the ST36 acupoint on both sides. The mouse ST36 is located 3–4 mm under the patella, between the fibula and tibia, and on the anterior side of the anterior tibial muscle. EA was performed using an electronic Trio 300 stimulator (Ito, Tokyo, Japan) with continuous square wave pulses of 1 mA intensity, 2 Hz frequency, and 150 μs pulse width for 20 min. During electrostimulation, slight twitching occurred in the muscles around the acupoint. EA was performed twice on Days 3 and 4 after FM induction.

4.3. Nociceptive Behavior Measurements

We first placed the mouse in an acrylic box above a wire mesh to facilitate pain testing. Mice were kept in a dark, noise-free, room-temperature environment to allow them to calm down and acclimatize for 30 min. Testing was conducted while the mice were inactive, not standing, not sleeping, not scratching, and not grooming. Mechanical and thermal pain were measured on Days 0, 3, and 4 before and after FM induction, to a total of three measurements. The pain threshold before ICS induction was used as baseline. We used electronic von Frey filaments for all tests 10 min apart (IITC Life Science Inc., Woodland Hills, CA, USA). We then used Hargreaves' test to measure the thermal withdrawal latency of the mouse paw to a radiant heat source using an IITC plantar analgesia device (SERIES8, Model 390G, IITC Life Science Inc., Woodland Hills, CA, USA). This device has a 20-s automatic power-off function to avoid injury to the mouse's hind paw.

4.4. Western Blot Analysis

The mouse cerebellum was dissected for protein extraction. Tissues were placed on ice and stored at −80ºC before protein extraction. Entire proteins were isolated in cold radioimmunoprecipitation (RIPA) lysis buffer containing 50 mM Tris-HCl pH 7.4, 250 mM NaCl, 1% NP-40, 5 mM EDTA, 50 mM NaF, 1 mM Na3VO4, 0.02% NaN3, and 1× protease inhibitor cocktail (AMRESCO). The extracted proteins were subjected to 8% SDS-Tris glycine gel electrophoresis and transmitted to a polyvinylidene difluoride (PVDF) membrane incubated first in 5% non-fat milk in TBS-T buffer (10 mM Tris pH 7.5, 100 mM NaCl, 0.1% Tween 20) before incubation with a primary antibody in TBS-T with 1% bovine serum albumin (BSA) for 1 h at room temperature. Peroxidase-conjugated antirabbit antibody or antimouse antibody (1: 5000) was used as secondary antibody. Blot bands were imagined using a chemiluminescent substrate kit (PIERCE) and LAS-3000 Fujifilm (Fuji Photo Film Co., Ltd., Tokyo, Japan). Where relevant, the protein concentration of the bands was measured using NIH Image J 1.54h software (Bethesda, MD, USA). β-actin or α-tubulin were used as internal control.

4.5. Immunofluorescence

Mice were euthanized with a 5% isoflurane and intracardially injected with 0.9% normal saline followed by 4% paraformaldehyde. Tissues were instantly excised and fixed with 4% paraformaldehyde at 4ºC for three days. Then, samples were embedded in 30% sucrose for cryoprotection overnight at 4ºC. Next, tissues were fixed in an optimal cutting temperature complex and quickly frozen in liquid nitrogen before storage at −80ºC. Frozen tissues were cut into a 20 mm sections using a cryostat directly placed on glass slides. The sections were fixed with 4% paraformaldehyde, and incubated with a blocking solution consisting of 3% BSA, 0.1% Triton X-100, and 0.02% sodium azide, for 1 h at room temperature. Then, samples were incubated overnight with the primary antibody (1:200, Alomone) for PD-L1 and TRPV1 in 1% BSA solution. Next, samples were

 doi:10.20944/preprints202601.0557.v1

incubated with the secondary antibody (1:500), 488-conjugated AffiniPure donkey antirabbit IgG (H + L) and 594-conjugated AffiniPure donkey antigoat IgG (H + L) for 2 h at room temperature before fixation with cover slips for immunofluorescence visualization.

4.6. Intracerebroventricular Injection

Mice were maintained under 1% isoflurane anesthesia and their heads fixed in a stereotaxic apparatus. A cannula, a 23-gauge 2-mm stainless steel tube, was inserted into the ventricle, secured, and placed subcortical at 0.5 mm in the anteroposterior axis, around 1 mm in the mediolateral axis, and about 2.5 mm in the dorsoventral axis and fixed to the skull with dental cement. After insertion into the ventricle, it was connected to a Hamilton syringe with a PE tube (PE10, Portex, Kent, UK). Using an injection pump (KD Scientific, Shanghai), 5 μg of PD-L1 or anti-PD-L1 neutralizing Ab (PD-L1 Ab; Sigma, USA) (2 μL/ventricle) was injected into the ventricle over 5 min. After injection, the cannula was maintained in the ventricle for 2 min to allow for continued PD-L1 or anti-PD-L1 neutralizing antibody diffusion.

4.7. Statistical Analysis

Statistical analysis was performed using the SPSS statistic program. All statistic data are presented as the mean ± standard error of mean. Differences among all groups were tested using an ANOVA test, followed by a post hoc Tukey's test. A $p < 0.05$ was considered to indicate statistical significance.

5. Conclusions

In sum, we for the first time clarified that the effect of EA, PD-L1 injection, and Trpv1 deletion in a FM pain model involved PD-1 and TRPV1 signaling. Interestingly, we validated that the antinociceptive effects of EA are mediated by PD-1/TRPV1 signaling pathway. The current features support the potential of EA as a therapeutic method for FM pain. Our results delivered their utility is importantly hindered in future clinical studies and serve EA as its therapeutic approaches for FM pain (Figure 9).

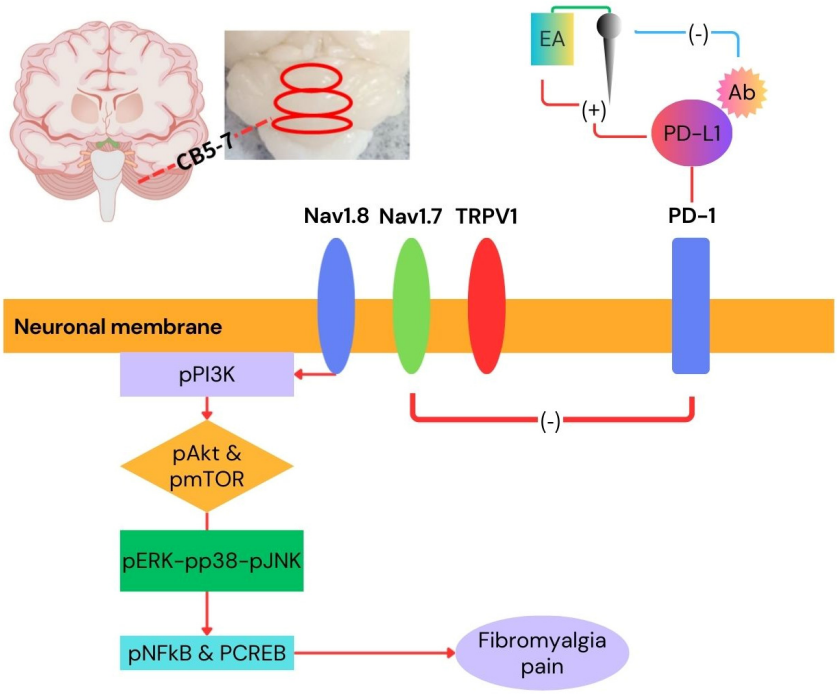

 doi:10.20944/preprints202601.0557.v1

Figure 9. Graphic diagram of EA in FM treatment via PD-1/TRPV1 and related molecules.

Main Findings and Implications

Our results mainly confirm the association between decreased PD-1 receptor expression and enhanced TRPV1-related pain kinase activity in the cerebellum of FM mice. EA or ICV injection of PD-L1 can alleviate FM pain by enhancing PD-1 receptor expression; similar results were observed in *Trpv1* knockout mice. ICV injection of PD-L1 neutralizing antibodies reversed these phenomena, confirming that the PD-1 receptor is the molecular mechanism of EA analgesia.

Study Strengths, Limitations, and Future Perspectives

EA precisely treats mice FM by activating PD-1 receptors. ICV administration of PD-L1 neutralizing antibodies reverses the analgesic effects of EA and PD-L1. These phenomena are attributed to the inhibition of TRPV pain-related molecular mechanisms by PD-1 receptors. Our study is limited by the fact that we only analyzed PD-1 receptors in the cerebellum of this model, and cannot rule out the involvement of other receptors. Clinical trials are necessary to confirm our findings.

Author Contributions: HY Huang, Y Chae, MC Lin, and IH Hsiao: Conceptualization, Methodology, Software, Data curation, Writing - original draft, Visualization, Investigation. HC Hsu, CY Ho, and YW Lin: Supervision, Validation, Writing - review & editing.

Funding: This work was supported by the following grants: NSTC 114-2314-B-039-031, NSTC 114-2314-B-039-087, CMU114-MF-111, and the "Chinese Medicine Research Center, China Medical University" from The Featured Areas Research Center Program within the framework of the Higher Education Sprout Project by the Ministry of Education (MOE) in Taiwan.

Institutional Review Board Statement: The animal study protocol was approved by the Institute of Animal Care and Use Committee of China Medical University (Permit no. CMUIACUC-2024-076, 12/12/2023).

Informed Consent Statement: Not applicable.

Data Availability Statement: The data that support the findings of this study are available on request from the corresponding author. The data are not publicly available due to privacy or ethical restrictions.

Conflicts of Interest: The authors declare no financial or other relationships that might lead to conflicts of interest.

References

1. Honjo, T. Seppuku and autoimmunity. *Science* **1992**, *258*, 591-592, doi:10.1126/science.1384132.
2. Ortega, M.A.; Boaru, D.L.; De Leon-Oliva, D.; Fraile-Martinez, O.; Garcia-Montero, C.; Rios, L.; Garrido-Gil, M.J.; Barrena-Blazquez, S.; Minaya-Bravo, A.M.; Rios-Parra, A.; et al. PD-1/PD-L1 axis: implications in immune regulation, cancer progression, and translational applications. *J Mol Med (Berl)* **2024**, *102*, 987-1000, doi:10.1007/s00109-024-02463-3.
3. Chen, G.; Kim, Y.H.; Li, H.; Luo, H.; Liu, D.L.; Zhang, Z.J.; Lay, M.; Chang, W.; Zhang, Y.Q.; Ji, R.R. PD-L1 inhibits acute and chronic pain by suppressing nociceptive neuron activity via PD-1. *Nat Neurosci* **2017**, *20*, 917-926, doi:10.1038/nn.4571.
4. Jurado-Priego, L.N.; Cueto-Urena, C.; Ramirez-Exposito, M.J.; Martinez-Martos, J.M. Fibromyalgia: A Review of the Pathophysiological Mechanisms and Multidisciplinary Treatment Strategies. *Biomedicines* **2024**, *12*, doi:10.3390/biomedicines12071543.
5. Tsamou, M.; Kremers, F.A.C.; Samaritakis, K.A.; Roggen, E.L. Identifying microRNAs Possibly Implicated in Myalgic Encephalomyelitis/Chronic Fatigue Syndrome and Fibromyalgia: A Review. *Int J Mol Sci* **2024**, *25*, doi:10.3390/ijms25179551.
6. Hudson, J.; Imamura, M.; Robertson, C.; Whibley, D.; Aucott, L.; Gillies, K.; Manson, P.; Dulake, D.; Abhishek, A.; Tang, N.K.Y.; et al. Effects of Pharmacologic and Nonpharmacologic Interventions for the

 doi:10.20944/preprints202601.0557.v1

Management of Sleep Problems in People With Fibromyalgia: Systematic Review and Network Meta-Analysis of Randomized Controlled Trials. *Arthritis Care Res (Hoboken)* **2025**, *77*, 1095-1105, doi:10.1002/acr.25505.

7. Rosenstrom, A.H.C.; Konsman, J.P.; Kosek, E. Cytokines in Cerebrospinal Fluid and Chronic Pain in Humans: Past, Present, and Future. *Neuroimmunomodulation* **2024**, *31*, 157-172, doi:10.1159/000540324.
8. Fan, Z.; Dou, B.; Wang, J.; Wu, Y.; Du, S.; Li, J.; Yao, K.; Li, Y.; Wang, S.; Gong, Y.; et al. Effects and mechanisms of acupuncture analgesia mediated by afferent nerves in acupoint microenvironments. *Front Neurosci* **2023**, *17*, 1239839, doi:10.3389/fnins.2023.1239839.
9. Torres-Rosas, R.; Yehia, G.; Pena, G.; Mishra, P.; del Rocio Thompson-Bonilla, M.; Moreno-Eutimio, M.A.; Arriaga-Pizano, L.A.; Isibasi, A.; Ulloa, L. Dopamine mediates vagal modulation of the immune system by electroacupuncture. *Nat Med* **2014**, *20*, 291-295, doi:10.1038/nm.3479.
10. Liu, S.; Wang, Z.; Su, Y.; Qi, L.; Yang, W.; Fu, M.; Jing, X.; Wang, Y.; Ma, Q. A neuroanatomical basis for electroacupuncture to drive the vagal-adrenal axis. *Nature* **2021**, *598*, 641-645, doi:10.1038/s41586-021-04001-4.
11. Hsiao, I.H.; Liao, H.Y.; Cheng, C.M.; Yen, C.M.; Lin, Y.W. Paper-Based Detection Device for Microenvironment Examination: Measuring Neurotransmitters and Cytokines in the Mice Acupoint. *Cells* **2022**, *11*, doi:10.3390/cells11182869.
12. Hsiao, I.H.; Liao, H.Y.; Lin, Y.W. Optogenetic modulation of electroacupuncture analgesia in a mouse inflammatory pain model. *Sci Rep* **2022**, *12*, 9067, doi:10.1038/s41598-022-12771-8.
13. Liao, H.Y.; Lin, Y.W. Electroacupuncture Attenuates Chronic Inflammatory Pain and Depression Comorbidity through Transient Receptor Potential V1 in the Brain. *Am J Chin Med* **2021**, *49*, 1417-1435, doi:10.1142/S0192415X2150066X.
14. Hsiao, I.H.; Yen, C.M.; Hsu, H.C.; Liao, H.Y.; Lin, Y.W. Chemogenetics Modulation of Electroacupuncture Analgesia in Mice Spared Nerve Injury-Induced Neuropathic Pain through TRPV1 Signaling Pathway. *Int J Mol Sci* **2024**, *25*, doi:10.3390/ijms25031771.
15. Hsiao, I.H.; Lin, M.C.; Hsu, H.C.; Chae, Y.; Su, Y.K.; Lin, Y.W. Chemogenetic Modulation of Electroacupuncture Analgesia in a Mouse Intermittent Cold Stress-Induced Fibromyalgia Model by Activating Cerebellum Cannabinoid Receptor 1 Expression and Signaling. *Life (Basel)* **2025**, *15*, doi:10.3390/life15091458.
16. Lin, H.C.; Park, H.J.; Liao, H.Y.; Chuang, K.T.; Lin, Y.W. Accurate Chemogenetics Determines Electroacupuncture Analgesia Through Increased CB1 to Suppress the TRPV1 Pathway in a Mouse Model of Fibromyalgia. *Life (Basel)* **2025**, *15*, doi:10.3390/life15050819.
17. Yeh, Y.A.; Hsu, H.C.; Lin, M.C.; Chen, T.S.; Lin, W.C.; Huang, H.M.; Lin, Y.W. Electroacupuncture Regulates Cannabinoid Receptor 1 Expression in a Mouse Fibromyalgia Model: Pharmacological and Chemogenetic Modulation. *Life (Basel)* **2024**, *14*, doi:10.3390/life14111499.
18. Ghowsi, M.; Qalekhani, F.; Farzaei, M.H.; Mahmudii, F.; Yousofvand, N.; Joshi, T. Inflammation, oxidative stress, insulin resistance, and hypertension as mediators for adverse effects of obesity on the brain: A review. Biomedicine **2021**, 11, 13–22.
19. Lin, Y.W.; Chou, A.I.W.; Su, H.; Su, K.P. Transient receptor potential V1 (TRPV1) modulates the therapeutic effects for comorbidity of pain and depression: The common molecular implication for electroacupuncture and omega-3 polyunsaturated fatty acids. *Brain Behav Immun* **2020**, *89*, 604-614, doi:10.1016/j.bbi.2020.06.033.
20. Lofgren, M.; Sandstrom, A.; Bileviciute-Ljungar, I.; Mannerkorpi, K.; Gerdle, B.; Ernberg, M.; Fransson, P.; Kosek, E. The effects of a 15-week physical exercise intervention on pain modulation in fibromyalgia: Increased pain-related processing within the cortico-striatal- occipital networks, but no improvement of exercise-induced hypoalgesia. *Neurobiol Pain* **2023**, *13*, 100114, doi:10.1016/j.ynpai.2023.100114.
21. Kim, H.; Kim, J.; Loggia, M.L.; Cahalan, C.; Garcia, R.G.; Vangel, M.G.; Wasan, A.D.; Edwards, R.R.; Napadow, V. Fibromyalgia is characterized by altered frontal and cerebellar structural covariance brain networks. *Neuroimage Clin* **2015**, *7*, 667-677, doi:10.1016/j.nicl.2015.02.022.
22. Mosch, B.; Hagena, V.; Herpertz, S.; Diers, M. Brain morphometric changes in fibromyalgia and the impact of psychometric and clinical factors: a volumetric and diffusion-tensor imaging study. *Arthritis Res Ther* **2023**, *25*, 81, doi:10.1186/s13075-023-03064-0.

 doi:10.20944/preprints202601.0557.v1

23. Liu, D.; Zhang, Y.; Zhao, J.; Liu, B.; Lin, C.; Yang, M.; Gu, J.; Jin, O. Alterations of the resting-state brain network connectivity and gray matter volume in patients with fibromyalgia in comparison to ankylosing spondylitis. *Sci Rep* **2024**, *14*, 29960, doi:10.1038/s41598-024-79246-w.
24. Tsai, S.T.; Yang, C.C.; Liao, H.Y.; Lin, Y.W. Electroacupuncture Reduces Fibromyalgia Pain via Neuronal/Microglial Inactivation and Toll-like Receptor 4 in the Mouse Brain: Precise Interpretation of Chemogenetics. *Biomedicines* **2024**, *12*, doi:10.3390/biomedicines12020387.
25. Deng, D.; Zhang, T.; Ma, L.; Zhao, W.; Huang, S.; Wang, K.; Shu, S.; Chen, X. PD-L1/PD-1 pathway: a potential neuroimmune target for pain relief. *Cell Biosci* **2024**, *14*, 51, doi:10.1186/s13578-024-01227-3.
26. Wanderley, C.W.S.; Maganin, A.G.M.; Adjafre, B.; Mendes, A.S.; Silva, C.E.A.; Quadros, A.U.; Luiz, J.P.M.; Silva, C.M.S.; Silva, N.R.; Oliveira, F.F.B.; et al. PD-1/PD-L1 Inhibition Enhances Chemotherapy-Induced Neuropathic Pain by Suppressing Neuroimmune Antinociceptive Signaling. *Cancer Immunol Res* **2022**, *10*, 1299-1308, doi:10.1158/2326-6066.CIR-22-0003.
27. Zhao, L.; Ma, Y.; Song, X.; Wu, Y.; Jin, P.; Chen, G. PD-1: A New Candidate Target for Analgesic Peptide Design. *J Pain* **2023**, *24*, 1142-1150, doi:10.1016/j.jpain.2023.02.002.
28. Zhao, L.; Luo, H.; Ma, Y.; Zhu, S.; Wu, Y.; Lu, M.; Yao, X.; Liu, X.; Chen, G. An analgesic peptide H-20 attenuates chronic pain via the PD-1 pathway with few adverse effects. *Proc Natl Acad Sci U S A* **2022**, *119*, e2204114119, doi:10.1073/pnas.2204114119.
29. Shi, S.; Han, Y.; Wang, D.; Guo, P.; Wang, J.; Ren, T.; Wang, W. PD-L1 and PD-1 expressed in trigeminal ganglia may inhibit pain in an acute migraine model. *Cephalalgia* **2020**, *40*, 288-298, doi:10.1177/0333102419883374.